Hongguang Li | Sukumaran Santhosh Babu | Sarah T. Turner
Dieter Neher | Martin J. Hollamby | Tomohiro Seki | Shiki Yagai
Yonekazu Deguchi | Helmuth Möhwald | Takashi Nakanishi

Alkylated-C60 based soft materials

regulation of selfassembly and optoelectronic properties by chain branching

Suggested citation referring to the original publication:
Journal of Materials Chemistry C 1 (2013), pp. 1943–1951
DOI http://dx.doi.org/10.1039/c3tc00066d

Journal of Materials Chemistry C

RSC Publishing

PAPER

View Article Online
View Journal | View Issue

Alkylated-C_{60} based soft materials: regulation of self-assembly and optoelectronic properties by chain branching†

Cite this: *J. Mater. Chem. C*, 2013, **1**, 1943

Hongguang Li,[ab] Sukumaran Santhosh Babu,[c] Sarah T. Turner,‡[d] Dieter Neher,[d] Martin J. Hollamby,[c] Tomohiro Seki,[e] Shiki Yagai,[e] Yonekazu Deguchi,[af] Helmuth Möhwald[a] and Takashi Nakanishi*[ac]

Derivatization of fullerene (C_{60}) with branched aliphatic chains softens C_{60}-based materials and enables the formation of thermotropic liquid crystals and room temperature nonvolatile liquids. This work demonstrates that by carefully tuning parameters such as type, number and substituent position of the branched chains, liquid crystalline C_{60} materials with mesophase temperatures suited for photovoltaic cell fabrication and room temperature nonvolatile liquid fullerenes with tunable viscosity can be obtained. In particular, compound **1**, with branched chains, exhibits a smectic liquid crystalline phase extending from 84 °C to room temperature. Analysis of bulk heterojunction (BHJ) organic solar cells with a *ca.* 100 nm active layer of compound **1** and poly(3-hexylthiophene) (P3HT) as an electron acceptor and an electron donor, respectively, reveals an improved performance (power conversion efficiency, PCE: 1.6 ± 0.1%) in comparison with another compound, **10** (PCE: 0.5 ± 0.1%). The latter, in contrast to **1**, carries linear aliphatic chains and thus forms a highly ordered solid lamellar phase at room temperature. The solar cell performance of **1** blended with P3HT approaches that of PCBM/P3HT for the same active layer thickness. This indicates that C_{60} derivatives bearing branched tails are a promising class of electron acceptors in soft (flexible) photovoltaic devices.

Received 10th January 2013
Accepted 16th January 2013

DOI: 10.1039/c3tc00066d

www.rsc.org/MaterialsC

1 Introduction

Renewable and economical energy sources are constantly in demand. Organic solar cells could make a feasible contribution to this requirement, due to the ease of device preparation in contrast to their inorganic counterparts. Specifically, bulk heterojunction (BHJ) organic solar cells have received considerable attention in recent years.[1] Due to their excellent electron accepting ability,[2] fullerenes are often used as the n-type organic semiconducting material in BHJ solar cells. In this context, a key step is the chemical modification of C_{60} to enhance its solubility in organic solvents, which facilitates cell fabrication by solution processing. Suitable functionalization of C_{60} and highly ordered C_{60} structures may also lead to an improved performance of solar cells through optimization of the bicontinuous phase-segregated network in the active layer. Fullerenes are also known as intriguing building blocks in versatile self-assembled architectures. Attachment of substituent groups to the C_{60} unit has induced the formation of a variety of self-organized structures,[3] including liquid crystals.[4] Such self-organized "soft" architectures, in contrast to "hard" single crystals,[5] are easier to handle and therefore permit more flexible device fabrication.

The performance of fullerenes in BHJ solar cells and their supramolecular chemistry will depend on the attached substituents. In recent years, C_{60} derivatives that bear aliphatic chains, *i.e.*, alkylated-fullerenes, have received considerable attention.[6,7] This type of C_{60} derivatives can be prepared in high yield in a few synthetic steps. They have a variety of interesting properties and are currently a focal point in the development of soft C_{60}-containing materials such as organogels[6b] and liquid crystals.[6c] Driven by the polarity difference between the C_{60} moiety and aliphatic chains,[7f] alkylated-fullerenes can exhibit versatile self-organized architectures. This

[a]*Max Planck Institute of Colloids and Interfaces, 14424 Potsdam, Germany*
[b]*Laboratory of Clean Energy Chemistry and Materials, Lanzhou Institute of Chemical Physics, Chinese Academy of Sciences, Lanzhou 730000, China*
[c]*National Institute for Materials Science (NIMS), 1-2-1 Sengen, Tsukuba 305-0047, Japan*
[d]*Institute of Physics and Astronomy, Potsdam University, D-14476 Potsdam, Germany*
[e]*Graduate School of Engineering, Chiba University, 1-33 Yayoi-cho, Inage-ku, Chiba 263-8522, Japan*
[f]*Gunma National College of Technology, 580 Toriba, Maebashi, Gunma 371-8530, Japan*

† Electronic supplementary information (ESI) available: Detailed synthetic procedures and NMR, additional experimental data including XRD, POM, TGA, detailed analysis of UV-vis and electrochemical measurements. See DOI: 10.1039/c3tc00066d

‡ Current address: Institute of Chemistry, Technical University of Berlin, 10623, Berlin, Germany.

"hydrophobic-amphiphilicity" is becoming a popular route to obtain various self-organized macroscopic objects.[8]

Among the factors that influence the self-assembly behavior and optoelectronic properties of alkylated-fullerenes, the molecular structure of the aliphatic chain itself is an important aspect.[6c,7c,9] It is well-known that branched chains have a significantly decreased crystallization tendency. This enhances the solubility of the molecules in solvents and induces their material softness, lowering their melting point. Specifically, the introduction of branched aliphatic chains has a pronounced influence on the self-organization of the molecules (as seen in thermotropic liquid crystals) and it can bring in new functionalities such as enhanced carrier mobility in π-conjugated systems.[9b,c] Therefore, our strategy is to replace the linear aliphatic chains (*e.g.* **10**, Fig. 1) in the C_{60} derivatives with branched ones (*e.g.* **1**). This approach should expand the opportunities to regulate and soften the self-assembly, while improving the performance in BHJ solar cells.

Here, we report the preparation of C_{60}-containing soft materials and the photovoltaic evaluations of a new library of alkylated-fullerenes that bear "branched" aliphatic chains. By optimizing the length and substituent positions of the branched aliphatic chains, we are able to construct soft materials such as smectic thermotropic liquid crystals and room temperature nonvolatile C_{60}-liquids. The C_{60} derivatives have high C_{60} contents up to 54%. As the strong crystallization tendency of C_{60} may lead to carrier transport trapping at defects when blended with the electron donor molecules such as poly(3-hexylthiophene) (P3HT), we propose that the softness of the branched alkyl chains can help to lower the crystallinity and to improve the charge transport capability. This makes such molecules good candidates for the preparation of organic solar cells with soft and flexible characteristics.

2 Results and discussion

2.1 Synthesis

The molecular structures of alkylated-fullerenes **1–9** which bear branched alkyl chains studied in this work are summarized in Fig. 1. In the current study, all the branched alkyl chains are racemic mixtures. The compounds were synthesized in three steps starting from branched alcohols. As a typical example, the synthetic route of **1** is given in the supporting information (ESI, Scheme S1†). For comparison, Fig. 1 also involves two reference C_{60} derivatives (**10**, **11**) bearing three eicosyloxy linear chains at the (3-, 4-, 5-)[7b] and (2-, 4-, 6-)[7a] substituent positions of the phenyl moiety, respectively. To minimize the formation of multiadducts on the C_{60} moiety, a 1.5 molar equivalent of pristine C_{60} is used in those syntheses. Using such a strategy, **1–9** were obtained with isolation yields up to 56.1% based on the benzaldehyde quantity. This good synthetic yield allows us to easily prepare more than one gram of the target compounds, permitting a deeper investigation of their bulk self-assembly behavior and assessment of photovoltaic performance.

2.2 Mesomorphic thermal behavior

Recently, considerable attention has been paid to linear alkylated C_{60} that exhibit liquid crystalline phases.[6c,7b,g,h] The driving force of liquid crystal formation is the mutual immiscibility of

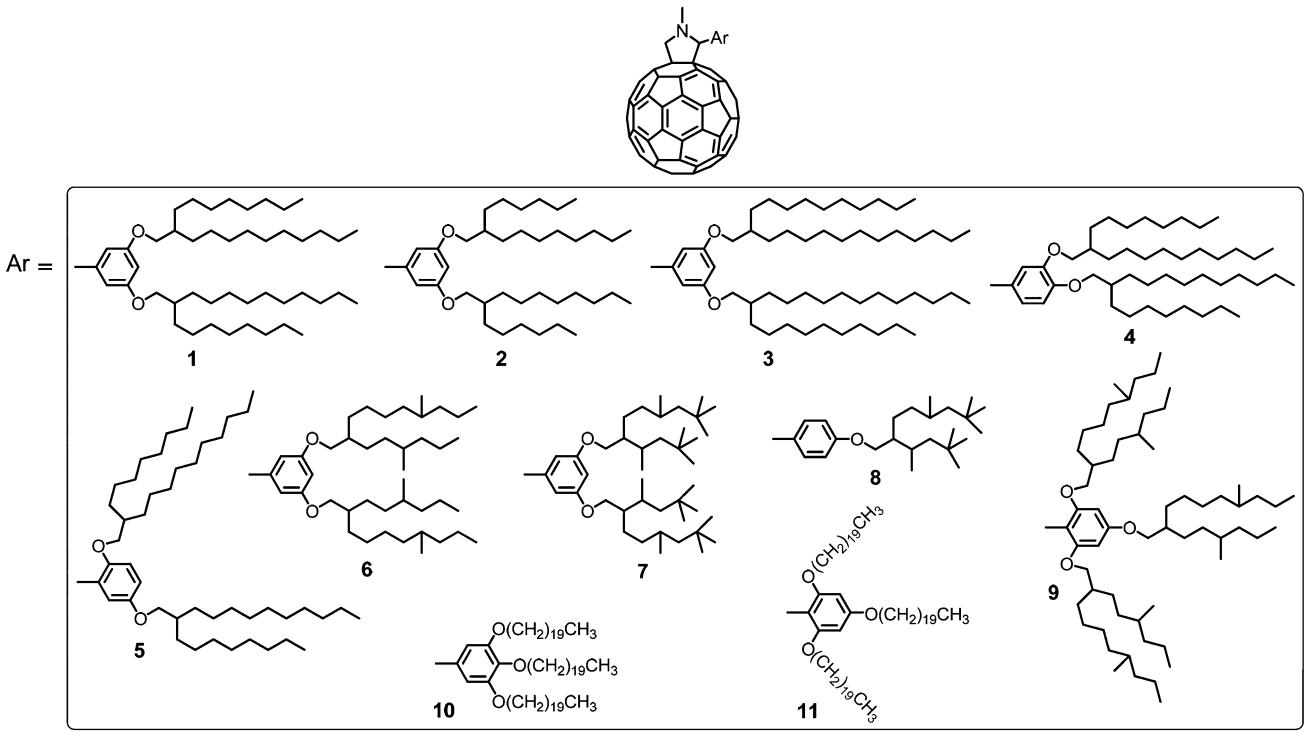

Fig. 1 Molecular structures of C_{60} derivatives bearing branched alkyl chains (**1–9**) newly investigated in this study and bearing linear alkyl chains (**10**, **11**) for use as their reference.

C_{60} and the aliphatic chains. Compared to the C_{60} liquid crystals with bulky mesogens,[4] alkylated C_{60}, especially the alkylated *N*-methylfulleropyrrolidines, have higher C_{60} contents and excellent functionalities such as good redox activity as well as high carrier mobility.[7b] With the current strategy, mesophase formation has been observed for C_{60} derivatives that bear swallow-tail type and hyperbranched chains, as will be presented in detail below.

2.2.1 Derivatives with swallow-tail type chains. Fig. 2 summarizes the differential scanning calorimetry (DSC) results and polarized optical microscopy (POM) observations of three liquid crystalline C_{60} derivatives (**1**, **2** and **4**). Compound **1** is substituted at (3-, 5-) positions of the phenyl group with two 2-octyldodecyloxy groups. DSC and POM revealed the existence of a smectic phase that extends from 84 °C to room temperature (Fig. 2a and d). The liquid crystalline behavior exhibited by **1** is quite striking, as replacing linear aliphatic chains with branched ones previously led to the elimination of the mesophases in alkylated pentaadducts of C_{60}.[6c] It was noted that the thermotropic behavior of **1** shows a remarkable supercooling effect. For instance, in the DSC thermogram, only a small endothermic peak ($\Delta H = 0.57$ kcal mol^{-1}) was observed during the heating process and no obvious peaks could be detected during the cooling process. In POM observations, after the temperature was decreased below 84 °C, it took a long time (over one hour) for the texture to appear, indicating that the self-organization of **1** is a slow process. Additionally, the thermotropic behavior is sensitive to the length of the grafted chains. Compound **2** with shorter 2-hexyldecyloxy groups exhibits a mesophase to isotropic phase transition at 148 °C (Fig. 2b and e, $\Delta H = 3.63$ kcal mol^{-1}). This large shift in the phase transition temperature highlights the stronger ability of the branched aliphatic chains to regulate the thermotropic behavior of alkylated fullerenes. Using linear aliphatic chains, an increase in the phase transition temperature of only 30 °C was previously noticed when the chain length was shortened.[7b]

Besides the chain length, the thermotropic behavior of the C_{60} derivatives can be tuned by the substitution positions of the tails. For example, when the substituted aliphatic chains of **1** were changed from the (3-, 5-) position to the (3-, 4-) position on the phenyl ring (**4**), an abrupt increase in the mesophase to isotropic phase transition temperature from 84 °C to 196.2 °C ($\Delta H = 4.48$ kcal mol^{-1}) was noticed together with the appearance of a crystal to mesophase transition at a temperature of 128.4 °C ($\Delta H = 0.52$ kcal mol^{-1}) as evidenced from Fig. 2c and f. This should be caused by densely packed alkyl chains, which exhibit a greater van der Waals interaction.[10] To characterize the organization of the liquid crystalline fullerenes, temperature-dependent X-ray diffraction (XRD) measurements were carried out on the mesophases of **1**, **2** and **4**. From Fig. 3, the organization of **1** in the mesophase can be assigned to a lamellar structure with an alternative interlayer distance of 3.50 nm, which is nearly double the molecular length of **1**. A small and broad peak at $2\theta \approx 8.0°$ (marked by ■) may originate from the organized C_{60} units with an average distance between adjacent C_{60}-cores of around 1 nm. This strongly supports the formation of a layer structure of the C_{60} moieties in the smectic mesophase of **1**. The halo centered at $2\theta \approx 19.6°$ originates from the molten aliphatic chains. For **2** and **4**, diffraction patterns characteristic of lamellar organizations were also obtained by XRD (Fig. S1 and S2†).

2.2.2 Derivatives with hyperbranched chains. Two different chains were chosen to investigate the influence of the branching degree of the grafted aliphatic chains on the mesomorphic behavior. These are denoted as hyperbranched aliphatic chain I (HBAC-I) used in compounds **6** and **9** and hyperbranched aliphatic chain II (HBAC-II) used in compounds **7** and **8**. Compound **6**, substituted at (3-, 5-) positions of the phenyl group with HBAC-I, exhibits two phase transitions at 57.4 and 111.4 °C, respectively (Fig. 4a). Interestingly, the lower temperature transition is exothermic instead of endothermic during

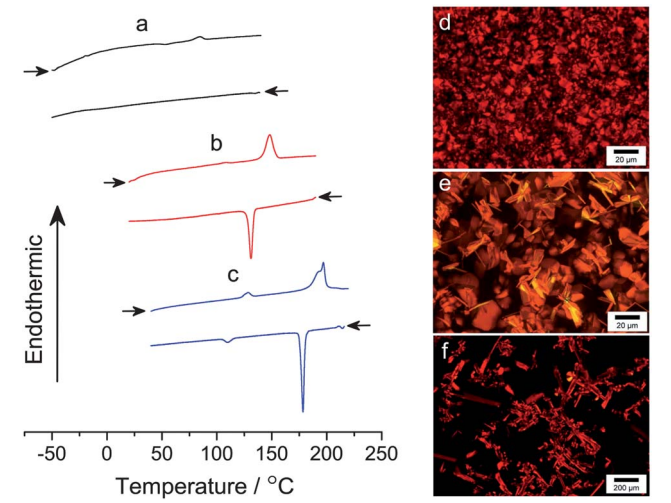

Fig. 2 DSC traces (a–c) from the second heating–cooling cycles and POM images (d–f) of **1** (a and d), **2** (b and e) and **4** (c and f) taken in their mesophases. Scan rates in the DSC are 10 °C min^{-1}.

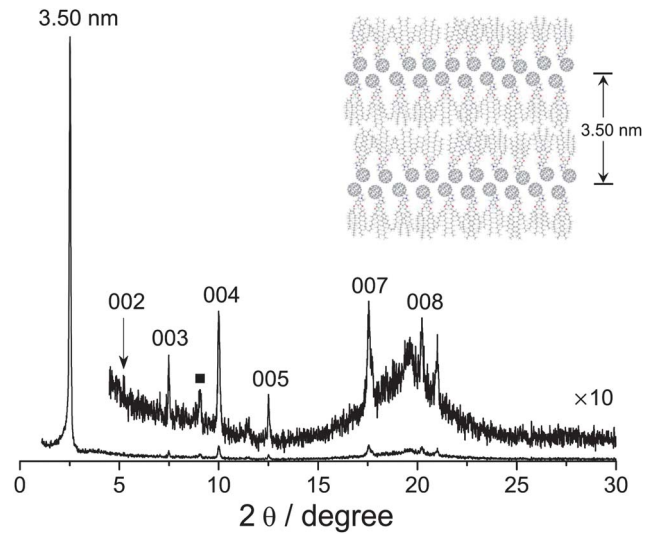

Fig. 3 XRD of **1** at 70 °C upon cooling from the isotropic phase at a speed of 0.1 °C min^{-1}. The organization of **1** can be described as a lamellar structure, as schematically shown in the inset.

the heating process. When heated to 120 °C which is above the melting point of **6**, a highly viscous isotropic phase formed. The sample was then cooled slowly (0.1 °C min^{-1}) to 100 °C and textures developed after aging for hours (Fig. 4d). This phenomenon together with the XRD results obtained both at 100 °C (Fig. 4c) and at room temperature (Fig. S3a and S3c†) provides strong evidence of α-crystal formation.[11]

Increasing the branching degree by changing HBAC-I to HBAC-II gives **7** which does not exhibit mesophases (Fig. 4b, S3b and S3d†). The viscosity of the isotropic phase (above 80 °C) of **7** is very high, which seems to originate from the presence of the hyperbranched aliphatic chains. This causes high intra- and intermolecular friction. It is reasonable to assume that the loss of the mesophase for **7** could be due to the two highly branched chains which are too bulky compared to the space occupied by the C_{60} moiety. To reduce the volume created by the aliphatic chains, only one HBAC-II was substituted at the (4-) position of the phenyl group (**8**). Compound **8** forms a shiny crystal at room temperature. XRD indicates that the self-organized structure of **8** in the crystalline form is indeed more ordered than that of **7** (Fig. S4a†). However, further investigations by DSC and POM (data not shown) reveal a very high (>300 °C) melting point and the absence of any mesomorphic phase. This is possibly due to the smaller grafted group insufficiently disturbing the strong π–π interactions between adjacent C_{60} molecules. When **8** was precipitated by adding excess methanol to a concentrated solution in dichloromethane, plate-like assembled structures were obtained (Fig. S4b†), similar to the objects obtained by a C_{60} derivative carrying a single linear alkyl chain but not like the well-developed 3-dimensional flowerlike microparticles seen from the alkylated fullerenes bearing two or three linear chains.[7e]

From the mesomorphic thermal property investigations, it can be concluded that the branched alkyl chains can soften self-organized objects formed from the alkylated fullerenes. This can be seen from the much lower phase transition temperatures of compounds functionalized with branched alkyl chains *versus* their saturated linear counterparts. Compared to the hyperbranched chains, swallow-tail type chains can more effectively adjust the π–π interaction between neighboring C_{60} units and van der Waals forces among alkyl chains, further softening the materials. By suitably modifying the chain length and the substitution position, liquid crystalline fullerenes with mesophase-to-isotropic phase transition temperature below 84 °C (such as **1**) can be obtained, opening the door for further photovoltaic evaluations using this intriguing family of alkylated-fullerenes (see Section 2.5).

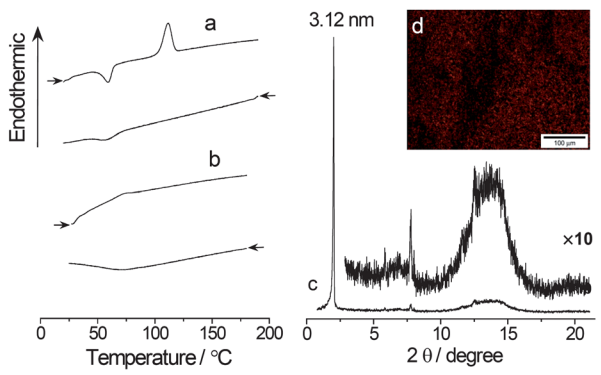

Fig. 4 DSC traces (a and b) from the second heating–cooling cycle of **6** (a) and **7** (b). XRD scattering peaks (c) and the POM image (d) of **6** upon cooling from the isotropic phase at a speed of 0.1 °C min^{-1}.

2.3 Room temperature liquid fullerenes

Due to the strong π–π interaction among adjacent C_{60} moieties, C_{60} and most of its derivatives are solids at room temperature. In recent years, there has been an increasing interest in π-conjugated molecules with fluid characteristics.[12] For alkylated fullerenes, the melting point depends on both van der Waals interaction of the aliphatic chains and π–π interaction among neighboring C_{60} molecules. As noted above, the substituted aliphatic chains can adjust the π–π interaction and decrease the melting point. For example, careful design previously led to the C_{60} derivative **11**, possessing a (2-, 4-, 6-) tris(eicosyloxy) phenyl group, which is a fluid at room temperature with a complex viscosity of approximately 1400 Pa s.[7a,i]

The melting point of a liquid material is also determined by factors other than intermolecular forces, such as the degree of molecular symmetry and the conformational degree of freedom.[13] In addition, the viscosity of the liquid is also directly related to the intermolecular forces upon flowing, *i.e.* the friction between molecules. Compared to linear chains, branched chains are expected to further lower the melting point and the viscosity. This is because both the van der Waals interaction of the substituted chains and the π–π interaction among C_{60} units will be significantly suppressed, leading to a weaker crystallinity of the molecule and a lower viscosity material. Indeed, substitution at (3-, 5-) positions of the phenyl group with two swallow-tail type alkyl chains, 2-decyltetradecyloxy, produces **3** as a solvent-free, nonvolatile, fluid material at room temperature. This is quite different from the case of derivatives that bear linear alkyl chains, for which a (2-, 4-, 6-) substitution pattern was needed to get room temperature C_{60}-liquids.[7a] No glassy transition could be detected from the DSC of **3** down to −120 °C (Fig. 5a). Rheological measurements verified the liquid character of **3**, where the viscous modulus (G'') is higher than the elastic modulus (G') within the investigated frequency range (Fig. 5d, black markers, a visual photo in an inset of Fig. 5d). If a (2-, 5-) substitution position is applied (*e.g.* **5**), the necessary aliphatic chain length, *i.e.*, 2-octyldodecyloxy, to produce a room temperature C_{60}-liquid is even shorter, which corresponds to a higher C_{60} content (49.8% by weight for **5** *versus* 46.2% for **3**). As with **3**, no clear glassy transition of **5** could be detected from DSC down to −120 °C (Fig. 5b). In addition, rheological measurements showed that G' and G'' of **5** (Fig. 5d, red markers) are smaller than those of **3**. Moreover, the complex viscosity (η^*) of **5** (~260 Pa s) is found to be one order of magnitude lower than that of **3** (~1500 Pa s) (Fig. 5e). This indicates that the (2-, 5-) substitution strategy, and in particular the introduction of the alkyloxy group at the 2-position of the phenyl ring, is more effective in producing less viscous C_{60}-liquids. Such a phenomenon could be due to an increasing

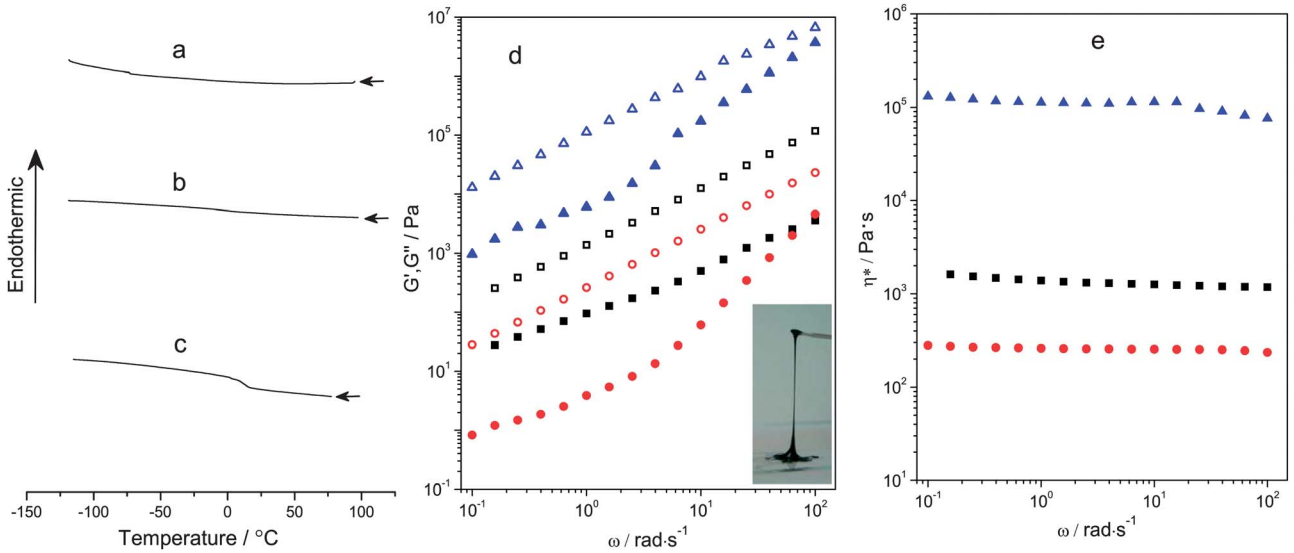

Fig. 5 DSC traces from the second cooling of **3** (a), **5** (b) and **9** (c). (d) Elastic modulus (solid symbols) and viscous modulus (open symbols) for **3** (black squares), **5** (red circles) and **9** (blue triangles) as a function of angular frequency under a constant strain amplitude of 0.5 at 20 °C. The inset is a typical image of **3** under mechanical pull at 20 °C. (e) Complex viscosity for **3** (black squares), **5** (red circles) and **9** (blue triangles) as a function of angular frequency under a constant strain amplitude of 0.5.

molecular asymmetry from **3** to **5**, which is consistent with the rule regulating the properties of other types of liquid materials such as ionic liquids.[13]

In studies of thermotropic liquid crystalline behavior we have seen that the alkylated-fullerenes bearing hyperbranched chains have higher viscosities in the isotropic phases at high temperature compared to those bearing swallow-tail type chains. In order to see whether this is also the case for room temperature C_{60}-liquids, **9** was prepared which was substituted at (2-, 4-, 6-) positions of the phenyl group with HBAC-I. DSC measurements revealed a glassy transition temperature around 12 °C (Fig. 5c). Rheological measurements showed that **9** has the highest G' and G'' (Fig. 5d, blue markers) as well as η^* (~128 000 Pa s) among all C_{60}-liquids tested (Fig. 5e). Additionally, the η^* of **9** is two orders of magnitude higher compared to **11** (ref. 7*a*) which was also substituted at (2-, 4-, 6-) positions but with linear chains. This could be due to the hyperbranched structure which induces high intra- and intermolecular friction upon flowing, consistent with the observations of the liquid crystalline phase. It is therefore clear that the melting point and viscosity of the alkylated-fullerenes can be effectively lowered by suitable chain branching and by breaking the molecular symmetry, but that too high a degree of branching again increases the viscosity of the fluid materials.

2.4 Spectroscopic and electrochemical properties

Spectroscopic and electrochemical studies can not only provide basic physicochemical information, but also advice for further photovoltaic evaluations of these newly synthesized molecules. Initially the absorption characteristics were investigated, which is a known precondition for a material to be utilized in photovoltaic devices. All of the investigated molecules, especially the room temperature C_{60}-liquids **3** and **5**, were found to be quite soluble in a variety of solvents including toluene, monochlorobenzene, benzene, chloroform, dichloromethane and tetrahydrofuran. For instance, the solubility of **3** in toluene can exceed 0.2 M. Even in *n*-alkanes such as *n*-hexane and *n*-decane, it still exhibits considerable solubility.[14] These *n*-alkanes, however, are generally regarded as poor solvents for pristine C_{60} as well as most of its derivatives. From UV-vis spectroscopy, strong absorption was observed in both the UV and visible wavelength regions and the molar absorption coefficient (ε) decreased significantly with increasing wavelength, which is consistent with the characteristic spectroscopic properties of C_{60} monoadducts.[15] Fig. S5A† shows a typical result of the UV-vis analysis of **1** in dichloromethane and detailed information on the absorption characteristics of **1–8** can be found in Table S1.†

FT-IR is a powerful tool to probe the conformation of the alkyl chains in their solvent-free states. Typically, from the location of the asymmetric and symmetric methylene stretching bands, the extent of crystallinity of the oligomethylene units can be inferred.[7e] While the bands for the derivative **10** that bears three linear eicosyl chains (shown as the dotted line in Fig. 6) were located at 2918 and 2849 cm^{-1}, respectively, those of all the C_{60} derivatives that bear branched aliphatic chains are broadened and shifted to higher wavenumbers. This result indicates that the branched aliphatic chains are in a disordered state and that the crystallinity is poorer. A closer investigation of the C_{60}-liquid samples **3** and **5** reveals that the methylene stretching bands are even broader. On the other hand, the liquid crystalline material **4**, which has a high melting point of 196.2 °C, has the sharpest bands at slightly higher wavenumbers. This reveals that the fluidity of the chains has a close correlation with the melting point of the alkylated fullerenes. When the derivatives show higher fluidity, *i.e.* lower crystallinity, their melting points are also lower. From Fig. 6, it can also be seen that the stretching bands of the methylene units

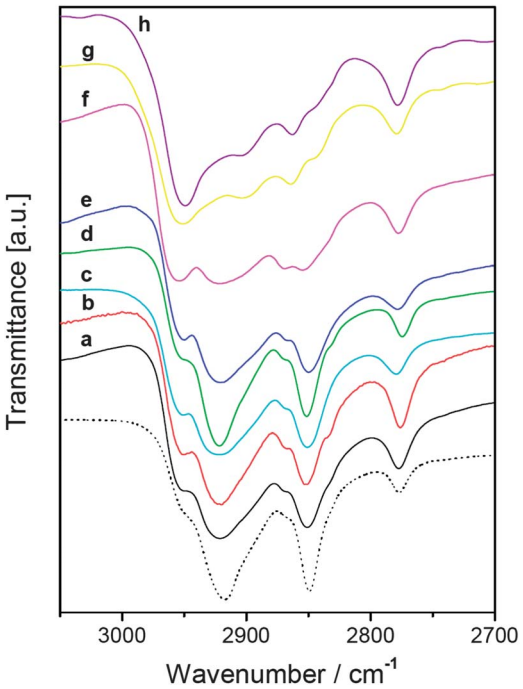

Fig. 6 FT-IR results of compounds **1–8**. Curves a–h correspond to the molecules **1–8** and a dotted line denotes the reference molecule **14** bearing three linear saturated eicosyl chains.

become less apparent while those from the terminal methyl groups become dominant for C_{60} derivatives modified with hyperbranched chains depending upon the $-CH_2-/-CH_3$ ratio.

It is known that pristine C_{60} can successively accept up to six electrons.[16a] The C_{60} monoadducts such as *N*-methylfulleropyrrolidines can retain the interesting electrochemical properties of the C_{60} unit.[16b,c] Rich electrochemical properties of compounds **1–8** were revealed by cyclic and differential pulse voltammetry measurements where three or four redox events have been observed (Fig. S5B, S5C and Table S2†). Although there are minor differences in their first redox potentials within 40 mV at around −1.17 V *versus* Fc/Fc^+, the redox properties of **1–8** are broadly similar. It is also noted that the redox properties of **1–8** are similar to those of other fullerene derivatives such as [6,6]-phenyl-C_{61}-butyric acid methylester (PCBM), with a first redox event at −1.17 V.[17] This indicates that the energy levels of the lowest unoccupied molecular orbitals (LUMO) of **1–8** and PCBM are also similar. Indeed, DFT calculations gave a LUMO energy level of −3.04 V for compound **1** and −3.13 V for PCBM.[18]

Combining the above results, it can be concluded that although the self-organization behavior of alkylated-fullerenes is highly dependent on the type, length and substitution position of the aliphatic chains, their spectroscopic and electrochemical properties in diluted solutions are mainly determined by the synthetic strategy of the C_{60} core,[16b,19] and show limited dependence on the aliphatic chains grafted on the phenyl group.

2.5 Bulk heterojunction organic solar cells

The observed properties of the branched-chain C_{60} derivatives, *e.g.* strong electron accepting ability, good thermal stability (Fig. S6†) and high solubility in organic solvents, are promising for applications in optoelectronic devices such as BHJ solar cells. To obtain a high power conversion efficiency (PCE), we envision that the C_{60} derivative used in the fabrication of the active layer should meet two main requirements. Firstly, an interpenetrated network should form where the C_{60} moieties have a long range order to facilitate the electron hopping and transport.[20] Secondly, the tendency of the C_{60} derivative to crystallize should not be too high as the formation of highly crystalline domains might introduce domain boundaries and deteriorate charge extraction. In order to improve the robustness of flexible organic solar cells for commercial applications, an enhanced degree of softness in the C_{60} derivatives is also an important consideration.[21] Based on these criteria, the liquid crystalline fullerenes reported here seem to be appropriate candidates. With a self-organized soft mesophase structure extending to room temperature and a moderate melting point of 84 °C, **1** was selected as a model alkylated-C_{60} derivative for evaluations in BHJ solar cells. P3HT was chosen as an electron donor molecule. The designed BHJ solar cell has a construction of ITO/PEDOT:PSS/active layer/samarium/aluminum, as illustrated in Scheme S2,† with an active layer thickness of 100 nm. At a **1**/P3HT weight ratio of 1 : 1, an open circuit voltage (V_{OC}) of 0.56 V, a short circuit current density (J_{SC}) of 5.5 mA cm^{-2} and a fill factor (FF) of 50% were obtained. This resulted in a PCE ($= V_{OC}J_{SC}FF/P_L$, where P_L is the incident radiant power of the light source) of 1.6 ± 0.1%. In the control experiment, PCBM, which is a standard soluble C_{60} derivative used in BHJ solar cells, was selected to replace **1**. In this case, V_{OC} was slightly lower but J_{SC} and FF were higher compared to the **1**/P3HT combination (Table 1). As a result, a slightly higher PCE of 2.2 ± 0.1% was obtained. Note that optimized P3HT:PCBM devices typically have blend layer thicknesses of 200 nm and above. Also noted is that the molecular weight of **1** (M_w = 1446.9) is higher than that of PCBM (M_w = 910.9) due to more substituted aliphatic chains. Thus at the same weight ratio of C_{60} derivative to P3HT, the C_{60} content of the **1**/P3HT blend (24.9%) is lower compared to that of the PCBM/P3HT mixture (39.6%). This may partially account for the slightly lower PCE for the **1**/P3HT blend. Some typical experimental results are summarized in Fig. 7. The functionality of the **1**/P3HT BHJ solar cell has been proven despite the slightly lower PCE than that of the PCBM/P3HT reference. In order to confirm the advantage of the liquid crystalline properties of the C_{60} acceptor in flexible organic solar cells, additional investigations are required. To meet this objective, optimized device parameters, including active layer thickness and its morphology, acceptor–donor ratios of the **1**/P3HT device as well as the application of derivative **2** are currently under investigation and will be reported elsewhere.

To obtain a deeper insight into the relationship between the molecular structure of the alkylated-fullerenes and their performance in BHJ solar cells, the performance of **10** which bears three linear aliphatic chains was evaluated. Although the V_{OC} is only slightly lower than that of the **1**/P3HT combination and the FF is even higher (Table 1), the performance of this solar cell significantly suffered from the low J_{SC} (2.0 mA cm^{-2}). As a result, a PCE of only 0.5 ± 0.1% was observed under the same experimental conditions. The much lower J_{SC} in the **10**/P3HT blend

Table 1 Parameters of BHJ solar cells fabricated using different C_{60} derivatives with P3HT[a]

Composition of the active layer	EQE (%) ± 2%	V_{OC} (V) ± 0.004 V	J_{SC} (mA cm^{-2}) ± 0.1 mA cm^{-2}	FF (%) ± 2%	PCE (%) ± 0.1%
1/P3HT	44	0.563	5.5	50	1.6
10/P3HT	17	0.460	2.0	56	0.5
PCBM/P3HT	49	0.488	6.6	65	2.2

[a] EQE: external quantum efficiency; V_{OC}: open circuit voltage; J_{SC}: short circuit current.

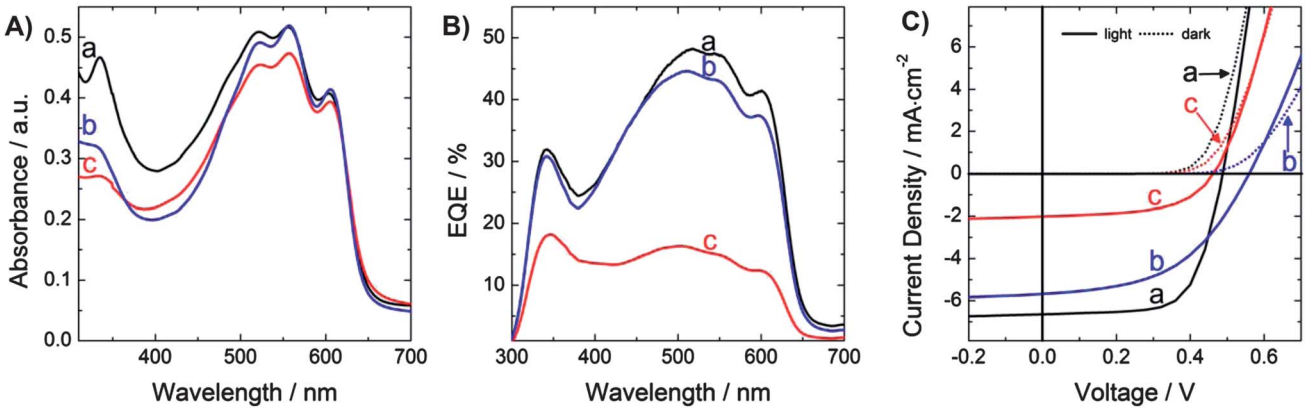

Fig. 7 (A) Standard absorption spectra of an active layer film with comparable thickness, (B) EQE and (C) *J*(*V*) curves of binary mixtures of P3HT/PCBM (curve a), P3HT/**1** (curve b) and P3HT/**10** (curve c), respectively. The weight ratio of P3HT to each C_{60} derivative is fixed at 1 : 1. The thickness of the active layer is 105 ± 5 nm.

could be due to the high crystallization tendency of **10**,[7e] which may prevent the formation of a co-continuous network of the donor and acceptor causing transport limitations. For example, unequal carrier mobility might reduce the photogenerated current due to space charge effects. This issue is the subject of future measurements under different driving and illumination conditions. We speculate that the improved performance of **1** compared to **10** is due to the presence of the branched aliphatic chains with liquid crystalline properties at room temperature. Although further structural analysis of the **1**/P3HT blend is needed, it could be inferred that with a long range order of the C_{60} moieties in the soft liquid crystalline material, the diffusion and charge separation of the excitons can be facilitated. Considering that the PCE of BHJ solar cells is also influenced by a variety of other factors including the solvent for cell fabrication,[22a] the mixing ratio of acceptor and donor molecules, the thickness of the active layer and the annealing temperature,[22b,c] the detailed mechanism is yet to be explored and the device performance is to be further optimized. Efforts in this direction are currently in progress and will be reported separately in the near future.

Conclusions

A new family of alkylated-C_{60} derivatives that bear branched aliphatic chains have been synthesized, and their self-assembly properties and BHJ solar cell performance have been investigated. By changing the chain structure and substitution position, the self-organization phenomena can be tuned. Compared to the linear chains, the branched counterparts have a larger capacity to control the self-assembly behavior. This can be seen from the formation of thermotropic smectic liquid crystals with a wide range of phase transition temperatures and solvent-free, nonvolatile, room temperature liquids with variable viscosity. In solvent-free conditions, the swallow-tail type branched chain derivatives are less viscous compared to the linear ones, which induces a weaker tendency of self-organization of the molecules. Functionalization with branched chains does not eliminate the intrinsic spectroscopic and electrochemical properties of the C_{60} units. This allows for interesting optoelectronic properties as demonstrated by the evaluations of BHJ solar cells. The formation of diverse self-organized structures would provide opportunities for further utilization of these intriguing compounds as building blocks for developments towards flexible-printable optoelectronic materials.

Acknowledgements

This work was supported by a Grant-in-Aid for Scientific Research on the Innovative Areas of "Emergence in Chemistry" (no. 2010) as well as for KAKENHI (23685033, 23111723) and PRESTO/JST (2007–2011) from the MEXT, Japan. We thank Prof. M. Funahashi (Kagawa Univ.), Prof. A. Saeki (Osaka Univ.), Prof. J. Wang (Sun Yat-sen Univ.), Dr R. Shomura and Dr M. Takeuchi (NIMS) for their meaningful discussions.

References

1 (*a*) G. Dennler, M. C. Scharber and C. J. Brabec, *Adv. Mater.*, 2009, **21**, 1323; (*b*) J. Peet, A. J. Heeger and G. C. Bazan, *Acc.*

Chem. Res., 2009, **42**, 1700; (*c*) P. Heremans, D. Cheyns and B. P. Rand, *Acc. Chem. Res.*, 2009, **42**, 1740; (*d*) D. Bagnis, L. Beverina, H. Huang, F. Silvestri, Y. Yao, H. Yan, G. A. Pagani, T. J. Marks and A. Facchetti, *J. Am. Chem. Soc.*, 2010, **132**, 4074; (*e*) H. Shang, H. Fan, Y. Liu, W. Hu, Y. Li and X. Zhan, *Adv. Mater.*, 2011, **23**, 1554; (*f*) H. M. Ko, H. Choi, S. Paek, K. Kim, K. Song, J. K. Lee and J. Ko, *J. Mater. Chem.*, 2011, **21**, 7248; (*g*) Y. Sun, G. C. Welch, W. L. Leong, C. J. Takacs, G. C. Bazan and A. J. Heeger, *Nat. Mater.*, 2012, **11**, 44.

2 (*a*) N. S. Sariciftci, L. Smilowitz, A. J. Heeger and F. Wudl, *Science*, 1992, **258**, 1474; (*b*) D. M. Guldi, B. M. Illescas, C. M. Atienza, M. Wielopolski and N. Martín, *Chem. Soc. Rev.*, 2009, **38**, 1587; (*c*) F. D'Souza and O. Ito, *Chem. Soc. Rev.*, 2012, **41**, 86; (*d*) C.-Z. Li, H.-L. Yip and A. K.-Y. Jen, *J. Mater. Chem.*, 2012, **22**, 4161.

3 (*a*) E.-Y. Zhang and C.-R. Wang, *Curr. Opin. Colloid Interface Sci.*, 2009, **14**, 148; (*b*) S. S. Babu, H. Möhwald and T. Nakanishi, *Chem. Soc. Rev.*, 2010, **39**, 4021.

4 (*a*) T. Chuard and R. Deschenaux, *Helv. Chim. Acta*, 1996, **79**, 736; (*b*) N. Maringa, J. Lenoble, B. Donnio, D. Guillon and R. Deschenaux, *J. Mater. Chem.*, 2008, **18**, 1524; (*c*) W.-S. Li, Y. Yamamoto, T. Fukushima, A. Saeki, S. Seki, S. Tagawa, H. Masunaga, S. Sasaki, M. Takata and T. Aida, *J. Am. Chem. Soc.*, 2008, **130**, 8886; (*d*) J. Vergara, J. Barberá, J. L. Serrano, M. B. Ros, N. Sebastián, R. Fuente, D. O. López, G. Fernández, L. Sánchez and N. Martín, *Angew. Chem., Int. Ed.*, 2011, **50**, 12523; (*e*) H. Mamlouk-Chaouachi, B. Heinrich, C. Bourgogne, D. Guillon, B. Donnio and D. Felder-Flesch, *J. Mater. Chem.*, 2011, **21**, 9121; (*f*) S. Campidelli, P. Bourgun, B. Guintchin, J. Furrer, H. Stoeckli-Evans, I. M. Saez, J. W. Goodby and R. Deschenaux, *J. Am. Chem. Soc.*, 2010, **132**, 3574; (*g*) D. Guillon, B. Donnio and R. Deschenaux, Liquid-Crystalline Fullerodendrimers and Fullero(Codendrimers), in *Fullerene Polymers: Synthesis, Properties and Applications*, ed. N. Marin and F. Giacalone, Wiley-VCH, Weinheim, 2009, pp. 247–270.

5 (*a*) H. X. Ji, J. S. Hu, Q. X. Tang, W. G. Song, C. R. Wang, W. P. Hu, L. J. Wan and S. T. Lee, *J. Phys. Chem. C*, 2007, **111**, 10498; (*b*) X. Zhang and M. Takeuchi, *Angew. Chem., Int. Ed.*, 2009, **48**, 9646; (*c*) C.-C. Chu, G. Raffy, D. Ray, A. D. Guerzo, B. Kauffmann, G. Wantz, L. Hirsch and D. M. Bassani, *J. Am. Chem. Soc.*, 2010, **132**, 12717; (*d*) S. S. Babu, A. Saeki, S. Seki, H. Möhwald and T. Nakanishi, *Phys. Chem. Chem. Phys.*, 2011, **13**, 4830.

6 (*a*) T. Nakanishi, M. Morita, H. Murakami, T. Sagara and N. Nakashima, *Chem.–Eur. J.*, 2002, **8**, 1641; (*b*) X. Yang, G. Zhang, J. Zhang, J. Xiang, G. Yang and D. Zhu, *Soft Matter*, 2011, **7**, 3592; (*c*) Y.-W. Zhong, Y. Matsuo and E. Nakamura, *J. Am. Chem. Soc.*, 2007, **129**, 3052; (*d*) H. Hotta, S. Kang, T. Umeyama, Y. Matano, K. Yoshida, S. Isoda and H. Imahori, *J. Phys. Chem. B*, 2005, **109**, 5700.

7 (*a*) T. Michinobu, T. Nakanishi, J. P. Hill, M. Funahashi and K. Ariga, *J. Am. Chem. Soc.*, 2006, **128**, 10384; (*b*) T. Nakanishi, Y. Shen, J. Wang, S. Yagai, M. Funahashi, T. Kato, P. Fernandes, H. Möhwald and D. G. Kurth, *J. Am. Chem. Soc.*, 2008, **130**, 9236; (*c*) J. Wang, Y. Shen, S. Kessel, P. Fernandes, K. Yoshida, S. Yagai, D. G. Kurth, H. Möhwald and T. Nakanishi, *Angew. Chem., Int. Ed.*, 2009, **48**, 2166; (*d*) T. Nakanishi, *Chem. Commun.*, 2010, **46**, 3425; (*e*) T. Nakanishi, Y. Shen, J. Wang, H. Li, P. Fernandes, K. Yoshida, S. Yagai, M. Takeuchi, K. Ariga, D. G. Kurth and H. Möhwald, *J. Mater. Chem.*, 2010, **20**, 1253; (*f*) H. Asanuma, H. Li, T. Nakanishi and H. Möhwald, *Chem.–Eur. J.*, 2010, **16**, 9330; (*g*) P. A. L. Fernandes, S. Yagai, H. Möhwald and T. Nakanishi, *Langmuir*, 2010, **26**, 4339; (*h*) H. Li, M. J. Hollamby, T. Seki, S. Yagai, H. Möhwald and T. Nakanishi, *Langmuir*, 2011, **27**, 7493; (*i*) T. J. Kramer, S. S. Babu, A. Saeki, S. Seki, J. Aimi and T. Nakanishi, *J. Mater. Chem.*, 2012, **22**, 22370.

8 (*a*) T. Lei and J. Pei, *J. Mater. Chem.*, 2012, **22**, 785; (*b*) F. Vera, M. Mas-Torrent, J. Esquena, C. Rovira, Y. Shen, T. Nakanishi and J. Veciana, *Chem. Sci.*, 2012, **3**, 1958.

9 (*a*) W. Pisula, M. Kastler, D. Wasserfallen, M. Mondeshki, J. Piris, I. Schnell and K. Müllen, *Chem. Mater.*, 2006, **18**, 3634; (*b*) X. Zhang, L. J. Richter, D. M. DeLongchamp, R. J. Kline, M. R. Hammond, I. McCulloch, M. Heeney, R. S. Ashraf, J. N. Smith, T. D. Anthopoulos, B. Schroeder, Y. H. Geerts, D. A. Fischer and M. F. Toney, *J. Am. Chem. Soc.*, 2011, **133**, 15073; (*c*) R. L. Uy, S. C. Price and W. You, *Macromol. Rapid Commun.*, 2012, **33**, 1162.

10 V. Percec, W.-D. Cho, G. Ungar and D. J. P. Yeardley, *J. Am. Chem. Soc.*, 2001, **123**, 1302.

11 (*a*) D. Kitagawa, I. Yamashita and S. Kobatake, *Chem. Commun.*, 2010, **46**, 3723; (*b*) J. Zhang, K. Tashiro, H. Tsuji and A. J. Domb, *Macromolecules*, 2008, **41**, 1352.

12 (*a*) S. S. Babu, J. Aimi, H. Ozawa, N. Shirahata, A. Saeki, S. Seki, A. Ajayaghosh, H. Möhwald and T. Nakanishi, *Angew. Chem., Int. Ed.*, 2012, **51**, 3391; (*b*) A. Nowak-Król, D. Gryko and D. T. Gryko, *Chem.–Asian J.*, 2010, **5**, 904; (*c*) S. Hirata, K. Kubota, H. H. Jung, O. Hirata, K. Goushi, M. Yahiro and C. Adachi, *Adv. Mater.*, 2011, **23**, 889; (*d*) E. M. Maya, J. S. Shirk, A. W. Snow and G. L. Roberts, *Chem. Commun.*, 2001, 615; (*e*) M. Brettreich, S. Burghardt, C. Böttcher, T. Bayerl, S. Bayerl and A. Hirsch, *Angew. Chem., Int. Ed.*, 2000, **39**, 1845.

13 T. Payagala, J. Huang, Z. S. Breitbach, P. S. Sharma and D. W. Armstrong, *Chem. Mater.*, 2007, **19**, 5848.

14 To be published elsewhere.

15 R. V. Bensasson, E. Bienvenüe, C. Fabre, J. M. Janot, E. J. Land, S. Leach, V. Leboulaire, A. Rassat, S. Roux and P. Seta, *Chem.–Eur. J.*, 1998, **4**, 270.

16 (*a*) Q. Xie, E. Pérez-Cordero and L. Echegoyen, *J. Am. Chem. Soc.*, 1992, **114**, 3978; (*b*) M. Prato and M. Maggini, *Acc. Chem. Res.*, 1998, **31**, 519; (*c*) S. Campidelli, J. Lenoble, J. Barberá, F. Paolucci, M. Marcaccio, D. Paolucci and R. Deschenaux, *Macromolecules*, 2005, **38**, 7915.

17 J. C. Hummelen, B. W. Knight, F. LePeq, F. Wudl, J. Yao and C. L. Wilkins, *J. Org. Chem.*, 1995, **60**, 532.

18 The calculation was made using DFT (B3LYP/6-31G*) method.

19 (*a*) M. Maggini, G. Scorrano and M. Prato, *J. Am. Chem. Soc.*, 1993, **115**, 9798; (*b*) B. I. Kharisov, O. V. Kharissova, M. J. Gomez and U. O. Mendez, *Ind. Eng. Chem. Res.*, 2009, **48**, 545.
20 Y. Matsuo, Y. Sato, T. Niinomi, I. Soga, H. Tanaka and E. Nakamura, *J. Am. Chem. Soc.*, 2009, **131**, 16048.
21 (*a*) M. V. Madsen, K. O. Sylvester-Hvid, B. Dastmalchi, K. Hingerl, K. Norrman, T. Tromholt, M. Manceau, D. Angmo and F. C. Krebs, *J. Phys. Chem. C*, 2011, **115**, 10817; (*b*) B. Omrane, C. K. Landrock, Y. Chuo, D. Hohertz, J. Aristizabal, B. Kaminska and K. L. Kavanagh, *Appl. Phys. Lett.*, 2011, **99**, 263305.
22 (*a*) G. Li, V. Shrotriya, J. Huang, Y. Yao, T. Moriarty, K. Emery and Y. Yang, *Nat. Mater.*, 2005, **4**, 864; (*b*) F. Padinger, R. S. Rittberger and N. S. Sariciftci, *Adv. Funct. Mater.*, 2003, **13**, 85; (*c*) P. Peumans, S. Uchida and S. R. Forrest, *Nature*, 2003, **425**, 158.